Calculation of Deflagrating Flame in a Rectangular Duct with Internal Solid Obstruction

S.S.Ibrahim, S.N.D.H. Patel, and G.K. Hargrave
Faculty of Engineering, Loughborough University, Loughborough, U.K.
Email: s.patel@lboro.ac.uk

Development of accurate models for the interaction between deflagrating flame and solid obstruction is still an area of active research. In this paper, results are presented from numerical calculations of turbulent flame propagation in an explosion combustion chamber (Hargrave et al., 2000). Stoichiometric mixture of methane-air was used to study the flame deflagration from a closed end of a rectangular (0.15×0.075m), 1m long open ended duct with a single built-in solid obstacle. Figure 1 shows a schematic of the experimental flame chamber setup. The rectangular obstacle is positioned across the duct cross-section at 0.15m from the ignition end, and its dimensions are 0.04×0.075×0.012m resulting in an area blockage of 50%.

Time dependent semi-implicit calculations were made to solve density weighted (Favre-averaged) conservation equations for mass, momentum, turbulence, reaction progress variable, $\tilde{c}$, and energy. A two equation eddy viscosity turbulence model (Launder and Spalding, 1972) modified for compressibility effects (Ahmadi-Befrui and Gosman, 1989) was used along with gradient transport assumption for turbulent diffusion to close the conservation equations. The equations were discretised with Euler implicit time and hybrid spatial differencing and the PISO solver due to Issa (1986) was used to solve the set of equations. The boundary conditions were of no flow at the closed end while a transmissive boundary condition was applied at the open end. Initial conditions were of no mean flow with a pre-set low level of turbulence kinetic energy and length scale. Typical calculation time step was of the order 10^{-6}s and the computational cell size ranged from 1.5×10^{-3}m to 2×10^{-3}m, which was found to provide grid independent solutions.

The mean rate of reaction, $\overline{\dot{\omega}}$, which was formulated as:

$$\overline{\dot{\omega}} = R\Sigma \tag{1}$$

where R is the local mean rate of reaction per unit surface area and Σ is the local mean surface area per unit volume of the flame. These two terms are expressed as (Bray, 1990):

$$R = \bar{\rho} \mathrm{u_L} I_o \tag{2}$$

$$\Sigma = \frac{g\bar{c}(1-\bar{c})}{|\sigma_y|\hat{L}_y} \tag{3}$$

where $\mathrm{u_L}$ is the laminar burning velocity, $\hat{L}_y$ is the flamelet wrinkling length scale, I_o is a factor correcting for mean effects of strain and curvature on the flamelet, g and $|\sigma_y|$ quantify the probability density function of the flamelet crossing process and the mean direction cosine

of the flamelet, respectively. The sensitivity of the controlling parameters g, $|\sigma_y|$, and $\hat{L}_y$ has been reported by Patel and Ibrahim (2000) using one-dimensional calculations, and for the present work the findings were applied to two-dimensional calculations. Therefore, g, $|\sigma_y|$, and $\hat{L}_y$ have been closed as (Patel and Ibrahim, 2000):

$$g = 1 + 2\widetilde{c} \tag{4}$$

$$|\sigma_y| = 0.65 \tag{5}$$

$$\hat{L}_y = C_L L_T \left(\frac{\mathrm{u_L}}{\mathrm{u'}} \right)^{(6D-13)} \tag{6}$$

where C_L is a constant of order unity, L_T is a scale of turbulence, and D is the fractal dimension computed from (North and Santavicca, 1992):

$$D = \frac{D_L}{\frac{\mathrm{u'}}{\mathrm{u_L}} + 1} + \frac{D_T}{\frac{\mathrm{u_L}}{\mathrm{u'}} + 1} \tag{7}$$

where D_L and D_T are the laminar and turbulent fractal dimensions taken to be equal to 2.19 and 2.32, respectively.

In the present work the initial flame kernel (ignition) was setup by allowing a gradient of the reaction progress variable to be established at the ignition point within time duration T_1. The transition to a highly turbulent flame following ignition over time T_1 is monitored through the relative magnitude between the turbulent, K_T, and laminar, K_L, flame stretch (Boudier et al., 1992):

$$\mathrm{K_L} = 2\frac{T_b}{T_u}\frac{\mathrm{u_L}}{r}, \qquad \mathrm{K_T} = \Gamma_{\overline{K}}\frac{\widetilde{\varepsilon}}{\widetilde{k}} \tag{8}$$

where $\Gamma_{\overline{K}}$ is the Intermittent Net Flame Stretch (ITNFS) function (Meneveau and Poinsot, 1991) and T is the temperature. The subscripts b and u denote burnt and unburnt mixture, respectively.

The formulated model we present in this paper found to produce results which are in good agreement with the experimental data reported by Hargrave and Williams (2000) at different stages of flame propagation following ignition. Figure 2 shows a comparison between predicted and experimental high speed flame images at different times after ignition. The notable convoluted flame structure observed in the experimental image at 38.9ms is not reproduced by the prediction. This can be attributed due to the fact that the experimental images are instantaneous while the predictions are based on Favre-averaged reaction progress

variable. The early stages of flame propagation is found to occur through a low level of turbulence which results in the laminar flame stretch becoming dominant. This is clearly illustrated through the variation of the relative ratio between the laminar and turbulent stretch, K_T / K_L, as shown in figure 3. As seen, the laminar stretch is higher than the turbulent value until about 14ms. As the flame approaches the solid obstacle (at about 26ms) it is found to decelerate, accelerate, and decelerate as it interacts with the solid obstruction, implying the effects of blockage, jetting through the clearance gaps, and reconnection, respectively. Comparison between calculated and measured values for flame speed as it interacts with the obstacle is shown in figure 4. The agreement obtained demonstrates the ability of the formulated model to satisfactorily reproduce flame acceleration and deceleration as it interacts with the solid obstacle.

The variation of the resulting pressure with time after ignition is shown in figure 5. As shown the occurrence of two pressure peaks has been observed from both experimental and calculated results. First peak pressure occurs during the first stage of flame propagation, from ignition until the flame reaches the obstacle. The second pressure peak occurs during the second stage of flame propagation from obstacle position until the flame reaches the open end, and is a result of burning the trapped mixture downstream from the obstacle.

In order to identify the regimes of combustion during flame propagation, field values for the flow Reynolds and Damköhler numbers have been calculated at different stages of flame propagation as shown in figure 6. The calculated values suggest that the combustion lies within the wrinkled and corrugated flamelet regimes as defined by Abraham et al. (1985).

It is concluded that the formulated model described in this paper predicts realistic results for flame deflagration over solid obstacle inside semi-confined chambers. The accuracy of the model was improved significantly when: 1) The transition from near laminar (early stages following ignition) to highly turbulent stretched flame is controlled through the laminar and turbulent stretch (eq. 8), and 2) The flamelet wrinkling length scale is properly related to the turbulence intensity and length scale (eq. 6).

References

[1] Abraham, J., Williams, F.A., and Bracco, F.V., SAE Paper 850345 (1985).

[2] Ahmadi-Befrui, B. and Gosman, A.D., *Int. Journal for Numerical Methods in Fluids*, 9, p.1073 (1989).

[3] Bray, K.N.C., *Proc. R. Soc. London, Ser. A*, 431, p. 315 (1990).

[4] Boudier, P., Henriot, S., Poinsot, T., and Baritaud, T., *24th Symp. (Int.) on Combustion*, The Combustion Institute, p. 503 (1992).

[5] Hargrave, G., and Williams, T.C., *9th Symp (Int.) on Flow Visualization*, Edinburgh (2000).

[6] Issa, R.I., *Journal of Comp. Phys.,* 62, p. 40 (1986).

[7] Launder, B.E., and Spalding, D.B., Academic Press, New York, p. 9 (1972).

[8] Meneveau C., and Poinsot, T., *Combust and Flame*, 86, p. 311 (1991).

[9] North, G.L. and Santavicca, D.A., *Combst. Sci. Technol.,* 72, p. 215 (1990).

[10] Patel, S.N.D.H., and Ibrahim, S.S., *Proc. of the 1st Int. Symp. on Turbulence and Shear Flow Phenomena,* (Santa Barbara) ed. Sanjoy Banerjee and John Eaton (Begell House Inc.), p. 1231 (1999).

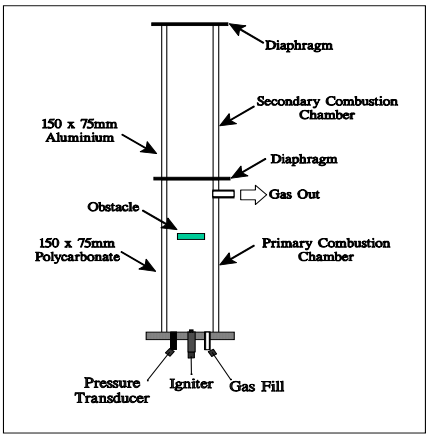

Figure 1: Schematic showing the experimental flame chamber

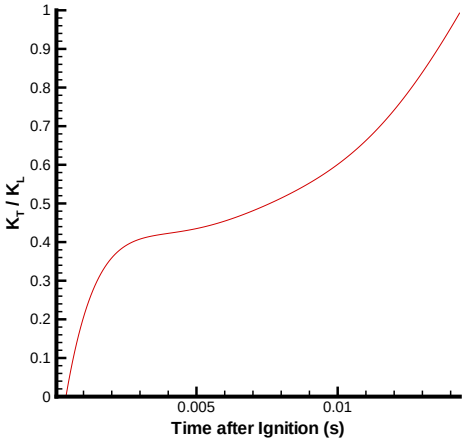

Figure 3: Calculated variation of turbulent to laminar flame stretch, K_T/K_L , with time (flame reaches obstacle at about 26ms)

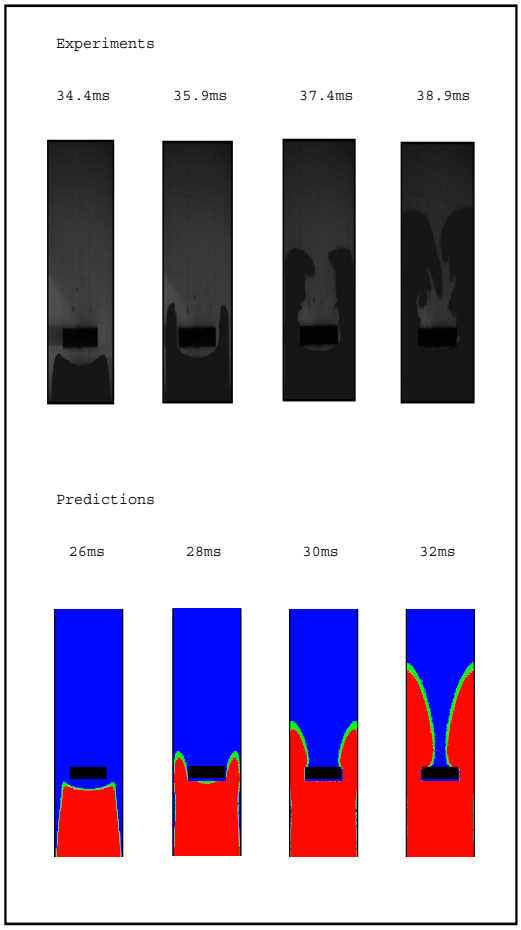

Figure 2: Comparison between calculated (Favre-averaged) and measured (instantaneous) flame shape images at different times after ignition

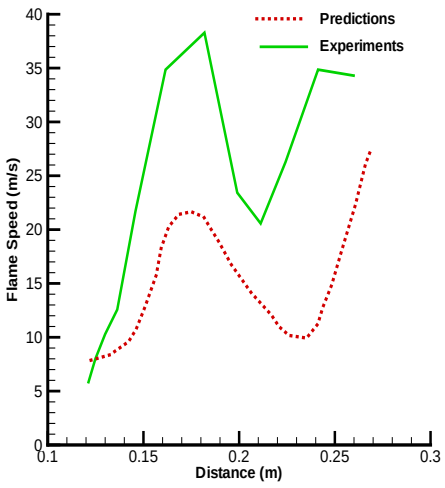

Figure 4: Comparison between calculated and measured flame speed vs. distance from ignition

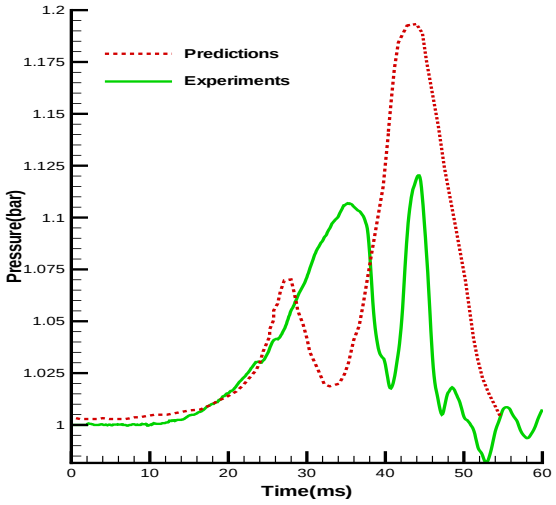

Figure 5: Comparison between calculated and measured pressure-time history

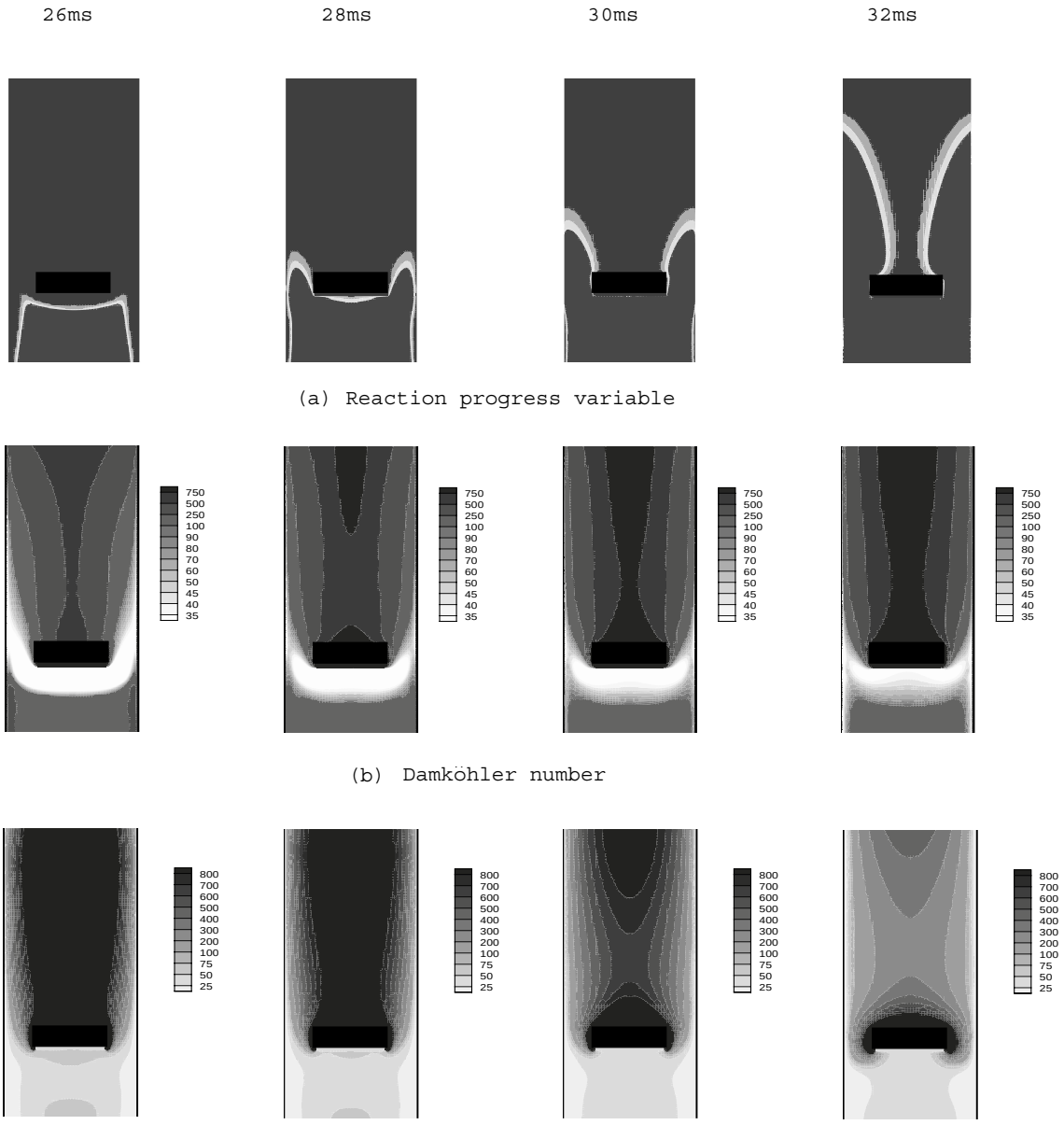

(a) Reaction progress variable

(b) Damköhler number

(c) Reynolds number

Figure 6: Evolution of (a) reaction progress variable, (b) Damkohler number, and (c) Reynolds number